



Membrane fouling control in anaerobic submerged membrane bioreactor

Mustafa Aslan^{a,*}, Yusuf Saatçi^b, Özge Hanay^b, Halil Hasar^{b,c}

^aDepartment of Environmental Engineering, Harran University, Osmanbey Campus, 63000 Sanliurfa, Turkey
Tel. +90 5372488105; email: mustafaaslan63@gmail.com

^bDepartment of Environmental Engineering, Firat University, 23119 Elazig, Turkey

^cNational Research Center on Membrane Technologies, Istanbul Technical University, 34469 Maslak, Istanbul, Turkey

Received 10 April 2013; Accepted 13 July 2013

ABSTRACT

In this study, the aim was to assess the impact of different membrane modules such as cylinder-shaped, funnel-shaped, and U-shaped on the membrane fouling behavior in a laboratory-scale submerged anaerobic membrane bioreactor (AnSMBR) treating the synthetic wastewater for over 124 days. A series of analysis, including soluble microbial products (SMP), extracellular polymeric substances (EPSs), scanning electron microscopy, energy dispersive X-ray spectroscopy, particle size distribution, and filtration resistances, was performed by considering all membrane modules. The results showed that difference between COD and TOC removals was negligible in membrane modules designed at different forms. However, the priority of the membrane modules in terms of providing high permeate fluxes was found to be cylinder-shaped > funnel-shaped > U-shaped bundle. Both SMP and EPS within cake formed on the fibers in the cylinder-shaped module were lower than those in the U-shaped and funnel-shaped modules. The particles in the U-shaped module were smaller than those in other modules while they were coarse in the cylinder-shaped module. The results demonstrate that cylinder-shaped module was the most suitable module of hollow fiber to control the membrane fouling in a AnSMBR.

Keywords: Submerged anaerobic membrane bioreactor; Membrane module type; Membrane fouling; SMP and EPS

1. Introduction

Submerged anaerobic membrane bioreactors (AnSMBRs) have been recently received increasing attention in treating various wastewater resulted from many municipal and industrial facilities due to the excellent effluent quality, less surplus sludge production, high treatment efficiency, net energy production,

low energy requirements, and small footprint [1–6]. Despite these advantages, membrane fouling is still one of the major limitations of AnSMBR technology in practical applications due to decrease in permeability and increase in operating and maintenance costs [7]. Unfortunately, it is unavoidable because a number of factors such as membrane flux, membrane pore size and materials, operation pressure and temperature, hydrodynamics and sludge characteristics including

*Corresponding author.

particle size, extracellular polymeric substances (EPSs), and soluble microbial products (SMP) have affected the membrane fouling mechanism [8–10]. Hence, various studies have been carried out to determine the correlation between membrane fouling and several operation parameters such as temperature [3], elevated pH [11], hydraulic retention time and solid retention time [10], membrane property [12], membrane configuration [13], sludge properties [14], and intermittent suction [6] in anaerobic membrane bioreactors. However, the effect of membrane properties on the membrane fouling has been recently investigated by using the polyacrylonitrile and polyvinylidene fluoride membranes in a submerged anaerobic/anoxic/oxic membrane bioreactor [12]. Although most of these studies are helpful, there is insufficient information related to the impact of membrane module design on the membrane fouling in AnSMBR.

In this study, the influence of different membrane modules on the mechanism of membrane fouling in terms of SMP, EPS, and particle size distribution (PSD) was investigated. Furthermore, scanning electron microscopy (SEM) images and elemental analysis of cake layer on membrane surfaces were evaluated in all membrane modules.

2. Materials and methods

2.1. Experimental setup

A schematic representation of AnSMBR was shown in Fig. 1. The reactor has a working volume of 24.5 l (diameter: 15 cm; and height: 50 cm) and was composed of two zones: (4.5 l) at the top zone, three hollow fiber microfiltration membrane modules were immersed and the bottom zone (20.5 l) was used as the sludge blanket. A mechanic stirrer (Thermolyne Cimarec, Model no: S47030) with 30 rpm was used for mixing the sludge liquor. Permeates were suctioned by peristaltic pumps with three heading (Watson Marlow 320S, UK), providing the required trans-membrane pressure (TMP). TMPs were measured by pressure sensors (AES sensors ATM, the Netherlands) in the permeate line. The membrane modules were U-shaped, cylinder-shaped, and funnel-shaped bundles of which were made of polyethylene (ZENA, Czech Republic) with a pore size of 0.1 μm and each comprised 60 fibers with a length of 9.5 cm. Each module has a membrane area of 54.2 cm^2 . Fig. 2 shows the membrane modul designs and shape of the reactor installation. The influent was pumped to the bottom zone by a feeding pump (Watson Marlow 320S). The temperature was kept stable at mesophilic condition

($37 \pm 2^\circ\text{C}$) by circulating warm water through the water jacket. Biogas production was measured with a wet gas meter.

2.2. Acclimation and synthetic wastewater

Inoculum with granular sludge was supplied from a full-scale reactor treating brewery wastewater. The initial granule concentration was 6.8 g VSS/l. The sludge volume index, density, and maximum specific methanogenic activity of the seed sludge were 8.62 ml/g TSS, 830 g/ml and 1.6 g CH_4 -COD/g VSS/d, respectively. The reactor was first filled with inoculums and synthetic wastewater at a ratio of 1:3. Membrane modules were located into anaerobic reactor after reaching the steady state on the 24th day, considering 90% COD removal and 0.301 CH_4/gCO_2 - $\text{D}_{\text{removed}}$. The main objective was to control membrane fouling. Therefore, in order to minimize fluctuations of wastewater characteristics, synthetic wastewater was used. The components (per liter water) present in synthetic wastewater were: 6 g sodium acetate (CH_3COONa), 1.35 g ammonium chloride (NH_4Cl), 355 mg potassium dihydrogen ortho-phosphate (KH_2PO_4), 384 mg magnesium sulfate (MgSO_4), 296 mg potassium chloride (KCl), 400 mg ethylene diamine triacetic acid (EDTA), 65.6 mg calcium chloride ($\text{CaCl}_2 \cdot 2\text{H}_2\text{O}$), 8.8 mg ammonium molybdate ($(\text{NH}_4)_6\text{Mo}_7\text{O}_{24} \cdot 4\text{H}_2\text{O}$), 14.4 mg copper sulfate ($\text{CuSO}_4 \cdot 5\text{H}_2\text{O}$), 40 mg iron sulfate ($\text{FeSO}_4 \cdot 7\text{H}_2\text{O}$), 12.8 mg cobalt chloride ($\text{CoCl}_2 \cdot 6\text{H}_2\text{O}$), and 176 mg zinc sulfate ($\text{ZnSO}_4 \cdot 7\text{H}_2\text{O}$). On the other hand, sodium bicarbonate (NaHCO_3), 250 mg/l, was consistently added to maintain pH at 7.0 ± 0.1 as a buffer, providing averaged values of 4,600 mg/l in COD, 1,465 mg/l in TOC, 1,200 mg/l in alkalinity, 132 mgHoAc/l in VFA, and 296/5.2/1 in COD/N/P in the influent.

2.3. Analysis

The COD, ammonium nitrogen ($\text{NH}_4\text{-N}$), total phosphorus, alkalinity, total suspended solids (TSSs), and volatile suspended solids (VSSs) were determined according to standard methods [15]. The pH was measured with a pH meter (Seven Multi, Mettler Toledo). Volatile fatty acids (VFAs) were measured by a spectrophotometer (Nova 60, Merck). TOC concentration and total nitrogen concentration were evaluated by a TOC analyzer (TOC-VCPH, Shimadzu). Methane fraction in the biogas was determined using a 2 m long and 3 mm i.d. stainless steel column of Porapak Q in a Shimadzu GC-14C gas chromatograph, equipped with a TC detector. The carrier gas was hydrogen at

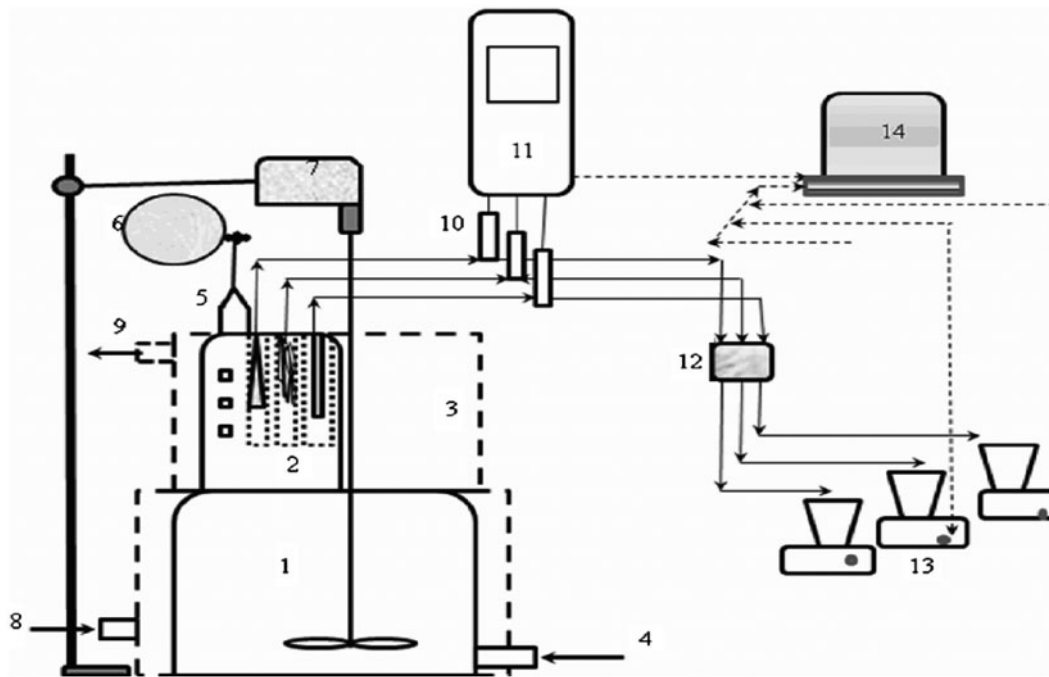


Fig. 1. A schematic diagram of SANMBR (1. Anaerobic reactor, 2. submerged membrane modules, 3. waterjacket system, 4. wastewater influent, 5. biogas effluent, 6. gas collection balloon, 7. mechanical mixer, 8. warm water influent, 9. warm water effluent, 10. pressure gauges, 11. command, 12. peristaltic pump, 13. on line scales, 14. computer).

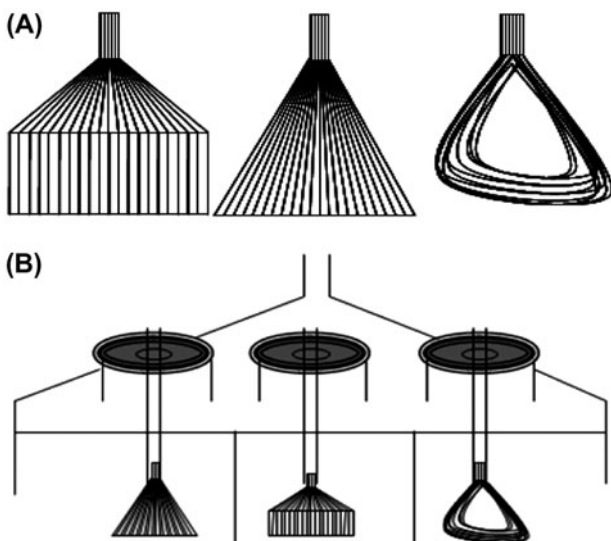


Fig. 2. (A) The membrane module designs; and (B) shape of the reactor installation.

15 ml/min. The oven, injector, and detector temperatures were set at 35, 110, and 110 °C, respectively.

SEM samples were fixed overnight at 40 °C in 3% glutaraldehyde and kept at pH 7.2 by a 0.1 M phosphate buffer. Samples were then dehydrated in a

graded ethanol/water series (10–30–50–70–90–100%) for 20 min at each concentration, and then dried for 5 h at 300 °C. Aqueous carbon was used to fix the specimens onto SEM mounts before gold sputter coating (30 mA for 2.5 min, vacuum 0.2 Torr). Samples were examined and photographed by a SEM (JEOL JSM-5610LV). The elements in cake layer were detected using a SEM coupled with an energy dispersive X-ray (EDX) spectroscopy (model JSM-840A).

2.4. EPS extraction and measurement

The extraction of SMP and EPS was based on a physical–chemical extraction (sodium hydroxide-formaldehyde) method [16]. SMP and EPS (or free EPS and bound EPS) were normalized as the sum of polysaccharide and protein, measured colorimetrically by the methods of Dubois et al. [17] and Lowery et al. [18], respectively. Bovine serum albumin was used as a protein standard, and glucose was used as a polysaccharide standard. Concentration of SMP and EPS in the anaerobic reactor was analyzed in the samples collected from the reactor with 20 days intervals during operation. In order to analyze the SMP and EPS in the cake layer, the membrane modules were first removed from the reactor after 124 days of operation time and then the cake sludge was carefully scraped off from

the membrane surface using a soft sponge followed by rinsing the deionized water.

2.5. PSD analysis

PSD of the sludge liquor was determined by a Malvern Mastersizer 2000 instrument with a detection range of 0.02–2,000 μm . The scattered light is detected by means of a detector that converts the signal to a size distribution based on volume. Each sample was measured three times with a standard deviation of 0.1–4.5%.

2.6. Membrane resistance

Membrane resistance was analyzed by Darcy's law as follows [14]:

$$R_t = R_m + R_c + R_p = \Delta P / J \times \eta \quad (1)$$

where R_t is the total hydraulic resistance, R_m is the membrane resistance, R_p is the pore blocking resistance, R_c is the cake layer resistance, ΔP is the transmembrane pressure, η is the dynamic viscosity, and J is the membrane flux. Each resistance value was determined on the different membrane modules used in the laboratory-scale AnSMBR. The procedure to determine each resistance value was reported by Lin et al. [14].

3. Results and discussion

3.1. System performance

pH and alkalinity of permeates and reactor varied in the range of 6.5–8 and 1,000–1,500 mg CaCO_3/l , respectively, which were suitable values for anaerobic wastewater treatment. The AnSMBR accomplished COD removal efficiencies between 97 and 98%, varying in the range of 120–420 mg/l in permeate. It was shown that the cylinder module was more effective when compared to the other modules although there was no significant difference in COD removal efficiencies for different membrane modules. Total organic carbon and sulfate concentrations in permeates were, respectively found in the range of 25–56 and 90–200 mg/l, and 96–98% and 38–65% in removal percentages. TSS and VSS concentrations in permeate were less than 10 mg/l that means removal efficiencies of 99%.

The membrane flux and the change in TMP are important to evaluate the performance of membrane bioreactor. Therefore, TMPs and flux values were simultaneously monitored in all modules throughout

the operation. In the most of previous studies, the behavior of membrane resistance and transmembrane pressure was investigated at stable flux [11,19] or the relationship between flux and membrane resistance was determined at a stable TMP [20–23]. In this study, we maintained TMP at a value of $170 \pm 3 \text{ mPa}$ to observe the effect of bio-fouling on membrane flux. It was shown that the flux decreased during the whole operation. In particular, an abrupt decrease in flux from 30 to about $5 \text{ l/m}^2 \text{ h}$ was monitored within the first 5 days of operation. Then, fluxes were gradually decreased to $1 \text{ l/m}^2 \text{ h}$ in funnel-shaped (F) and U-shaped (U) and $2 \text{ l/m}^2 \text{ h}$ in cylinder-shaped (C) modules within 124 days, as seen in Fig. 3. Our results are consistent with findings reported by Choo and Lee [24]. They observed that membrane flux was $20 \text{ l/m}^2 \text{ h}$ in the beginning of the operation of anaerobic membrane bioreactor using the ceramic membrane while it decreased to $1 \text{ l/m}^2 \text{ h}$ after 200 days. Similarly, Lin et al. [14] and Trzcinski and Stuckey [25] also reported the same behavior in the flux profiles in AnSMBR. In the present study, while hydraulic retention time was 2.67 days in the beginning of experiment, this value prolonged to 22 days due to the decrease in total flux. The permeate fluxes in the cylinder-shaped module were higher than those in the other modules. Priority of the membrane modules in terms of providing high permeate fluxes was found to be cylinder > funnel-shaped > U-shaped bundle. On the other hand, total resistances were directly calculated from the permeate fluxes as TMPs were kept stable. Due to the fact that the distance between each membrane fibers was 1 mm in cylinder membrane module and located vertically, the cake layer on the membrane surface was thinner than those in different modules. In addition, the fibers in cylinder-shaped bundle did not adhere or get close to each other due to its geometric shape. On the other hand, similarly the distance between each fibers of

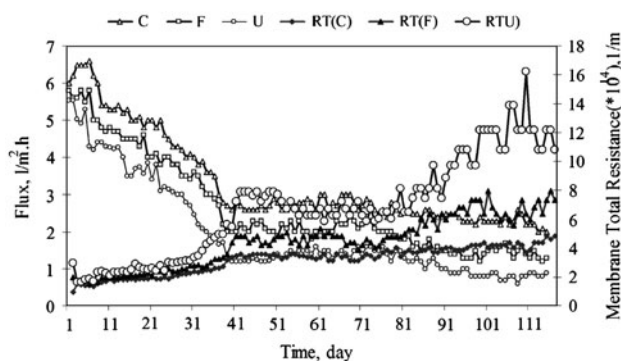


Fig. 3. The profiles of flux and total resistance during operation.

funnel-shaped module was 1 mm but the adherence of fibers occurred especially on the top part of module; hence, the cake layer on the membrane surface continuously enhanced. There was no measurable distance between fibers in U-shaped module; hence, the membrane fouling rapidly occurred and the cake thickness of the membrane surface was the highest when compared those in different modules.

The resistances from membrane fouling increased through the operation for 124 days as permeate fluxes decreased in all modules. The membrane resistance was found to be highest for U-shaped module followed by, respectively funnel-shaped and cylinder-shaped modules. As a result, the cylinder-shaped module provided high flux with related to module geometry because the cake resistance in cylinder membrane was low. The results showed that cylinder membrane module was more effective than other modules to control the membrane fouling and/or more sustainable operation.

It was shown that the major membrane resistance resulted from the cake resistance, varying in the range of 75–90% of total filtration resistance, which means a reversible fouling significantly by mechanical cleaning procedures. The resistance from pore blocking was determined in the range of 12–25%. The cake layer resistances were $8.24 \times 10^{+13}$, $13.3 \times 10^{+13}$, and $14.9 \times 10^{+13}$ for cylinder-shaped (C), funnel-shaped (F) and U-shaped (U) modules, respectively. Highest value for R_c was determined in the case of U-shaped module. This demonstrates that a rapid membrane clogging occurred in U-shaped module when compared with other modules (Fig. 4). These results also showed that cylinder membrane module is advisable to control the membrane fouling.

3.2. SMP and EPS content

Previous studies reported that SMP demonstrated considerable influence on membrane fouling [26–28]. For example, Tsuneda et al. [29] reported that sludge adhesion was enhanced by polymeric interactions when the EPS content increased. Pollice et al. [30] emphasized that fouling under subcritical flux operation was mainly caused by the accumulation of SMP and EPS in the pores and/or on the membrane surface. In present study, the concentrations of SMP and EPS changed in the range of 16–119 mg/l and 66–160 mg/l, respectively. Concentration profiles of SMP and EPS were observed as a contrasting direction to each other in the form of obvious three stages. SMP increased from about 20 mg/l at 40th day to 119 mg/l at 60th day as it decreased to about 50 mg/l at 80th

day. On the other hand, EPS decreased dramatically from 100 mg/l at 40th day to 65 mg/l at 60th day as it quickly increased to 160 mg/l at 80 day, as seen in Table 1. The results showed that, in agreement with previous studies, a higher SMP content corresponded to a higher filtration resistance. EPSs are also usually reported as a controlling factor of membrane fouling in MBRs. The results in the literature suggest that the role of EPS in membrane fouling rate is complex and depends on the changes in the dominant factors under different conditions.

SMP and EPS in the cake layer were, respectively 45 and 56 mg/l in the cylinder-shaped module (C), 175 and 180 mg/l in the funnel-shaped module (F) and 151, and 159 mg/l in the U-shaped module (U), as seen in Table 1. Both SMP and EPS in cylinder-shaped module were lower than the corresponding values of U-shaped and funnel-shaped modules. On the other hand, the cylinder-shaped module has an important attention because it has also the highest permeability and lowest membrane resistance. The results obtained from three different modules were in agreement with SMP and EPS contents when compared in term of fouling. In the literature, no references have been found about concerning the influence of membrane module design on bio-fouling in terms of SMP and EPS contents. However, these results demonstrated that membrane module design has a significant impact on the membrane fouling.

3.3. SEM–EDX

Fig. 4(A) indicates the SEM images of the membrane surface and EDX results (Fig. 5) for clean membrane used in this study. The cake layers in all the modules seem to be composed of both gel-like substances and sludge depositions (Fig. 4(B)–(D)). The cake layers were: (i) loose sludge depositions in the cylinder-shaped module (Fig. 4(B)), (ii) porous and modest compressed sludge depositions in the funnel-shaped module (Fig. 4(C)), and (iii) dense and compressed sludge depositions in the U-shaped module (Fig. 4(D)). The growth of a dense and compressed cake layer would certainly increase filtration resistance. This observation by using SEM images was in agreement with the TMP and flux profile. It was seen that both cake layer and crystal layer have significantly performed on the membrane surface in U-shaped module. The gel layer performed on outer of membrane surface was partially removed by physical cleaning (Fig. 4(E)–(G)). Considering the EDX images of membrane modules, the order of the contents of Ca, P, Zn, and S in three different modules is: cylin-

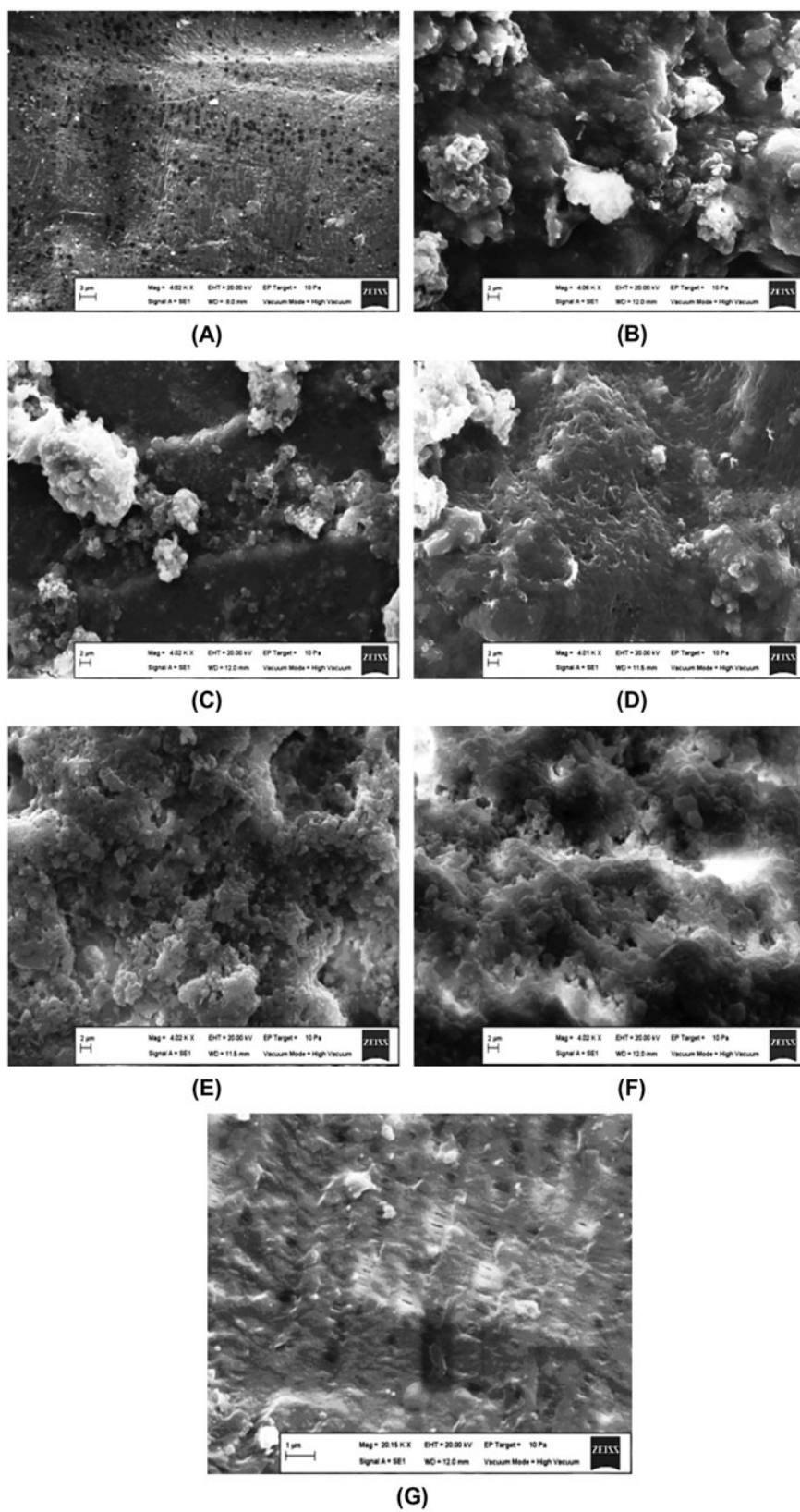


Fig. 4. SEM images: (A) clean membrane, cake layer images; (B) cylinder; (C) funnel-shaped; (D) U-bundle-shaped and SEM images after scrapping the cake layer; (E) cylinder; (F) funnel-shaped; and (G) U-bundle-shaped.

Table 1
SMP and EPS data in AnSMBR system and fouled membrane surfaces

Time, day	SMP, mg/l	EPS, mg/l	SMP, mg/g SS	EPS, mg/g SS
System sludge				
4	102.31	192.02	20.46	38.40
19	16.03	105.24	2.76	18.15
33	73.96	192.26	10.13	26.34
40	26.42	101.76	4.19	16.15
41	91.36	145.35	11.71	18.63
48	82.85	127.95	10.90	16.84
55	118.02	66.17	15.33	8.59
63	120.45	119.99	15.64	15.58
77	51.74	160.25	7.29	22.57
111	57.17	123.24	11.67	25.15
124	119.20	109.03	19.87	18.17
Fouled membrane surface				
Module				
C	45.49	55.94	2.27	2.80
F	174.88	180.04	8.4	9.00
U	150.88	158.63	7.54	7.93

der>funnel>U shaped modules (Fig. 6). This can be explained that the fouling on membrane surface was removed efficiently with physical cleaning in U-shaped module. Additionally, the inorganic structure could not be removed in cylinder- and funnel-shaped modules (Fig. 7). Since there is insufficient information on the effects of membrane modules on controlling

membrane fouling, it is expected that these results will highlight to further researches.

Energy dispersive spectrum analysis indicated the presence of C, O, Na, Mg, Al, S, Si, P, K, Ca, Zn, Cl, and Fe in the sludge cake layer. The contents of Ca, Mg, Fe, and P were higher in cylinder- and funnel-shaped modules than those in U-shaped modules. However, bio-fouling was significantly performed on U-shaped module. The increase of those elements may result in crystal generation from mineral sources. Our results are consistent with findings by Dagnew [31]. Metal carbonates such as Ca, Mg, and Fe may enhance the potential of membrane scaling and precipitate biopolymers containing ionizable groups such as CO_3^{2-} , SO_4^{2-} , PO_4^{3-} , OH^- , and COO^- . The groups consisted calcium and acidic functional may perform complexes and improve a biosludge layer and gel layer which hinder the flux fall. According to our results, it was evaluated that the complex structures resulted from both inorganic pollutants and biopolymer have significantly decreased the permeate fluxes and consequently membrane permeability. The membrane fouling resistances of all membrane modules were found to be very high while the pore blocking resistances (R_p) were low. The resistance from pore blocking was determined in the range of 8–15% while the cake layer resistance (R_c) was in the range of 85–92% in the modules. It was also assigned that the inorganic precipitation coupled the organic foulants would cause the membrane fouling problem in AnSMBR. In addition, the content of organic substances was found to be lower for U-shaped module than those for the others. In parallel with these findings, the cake layer

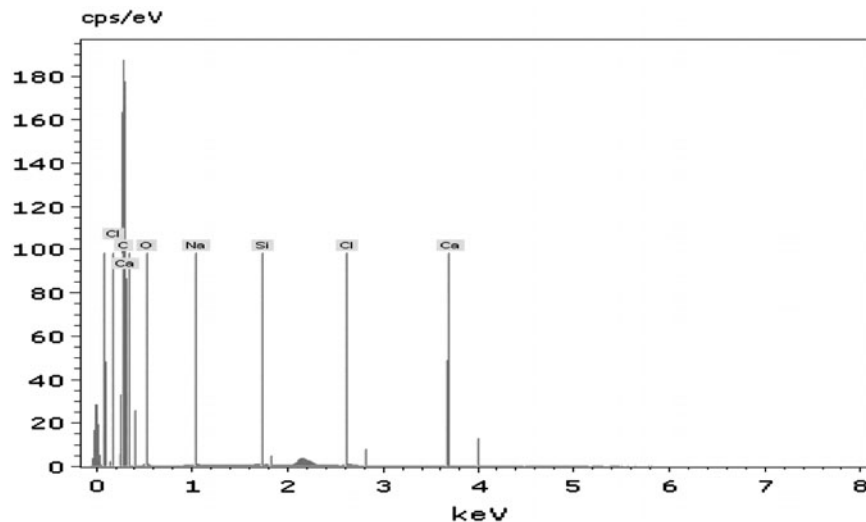


Fig. 5. EDX analysis of clean membrane.

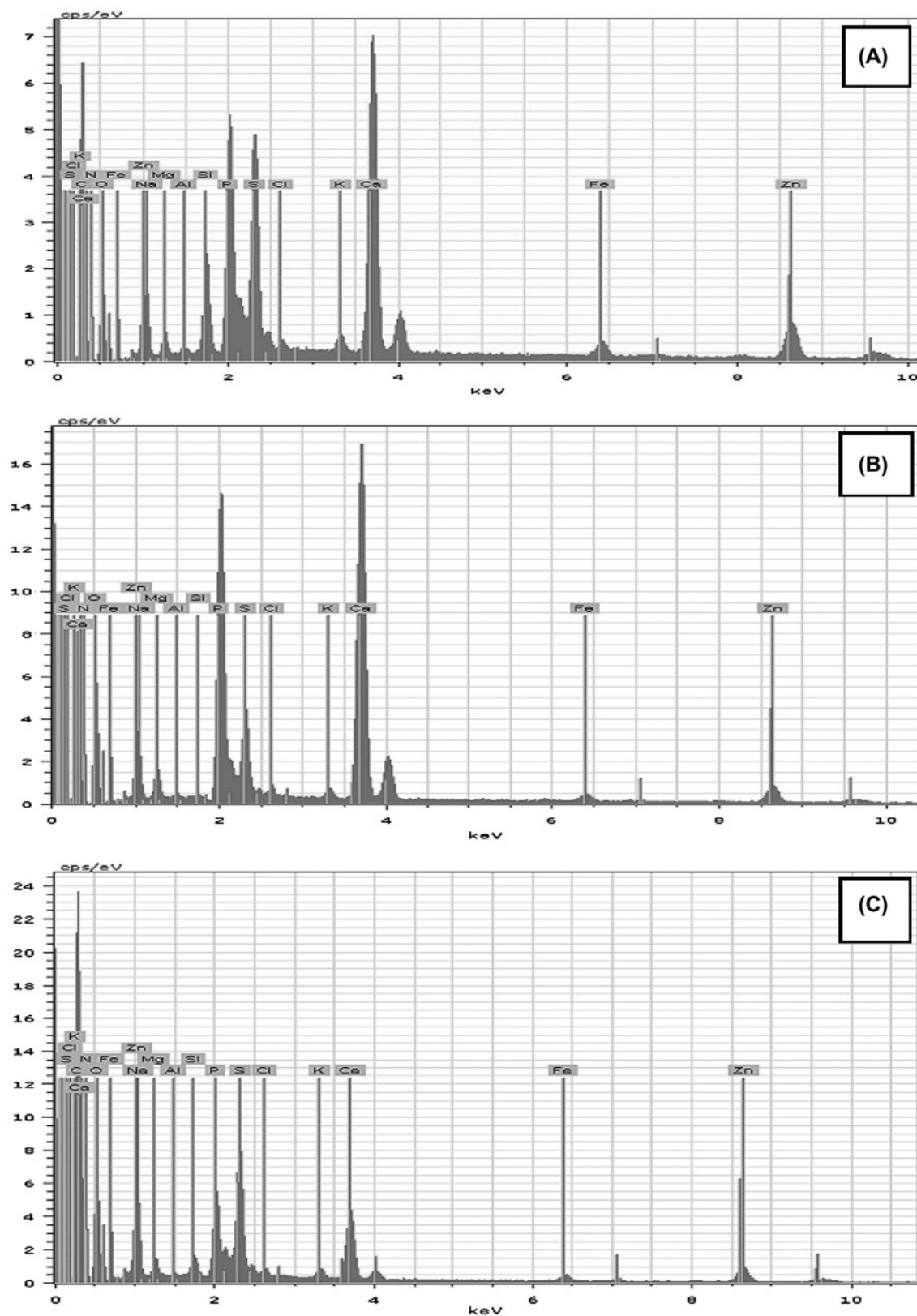


Fig. 6. EDX analysis of cake layer images; A: cylinder, B: funnel shaped and C: U bundle shaped.

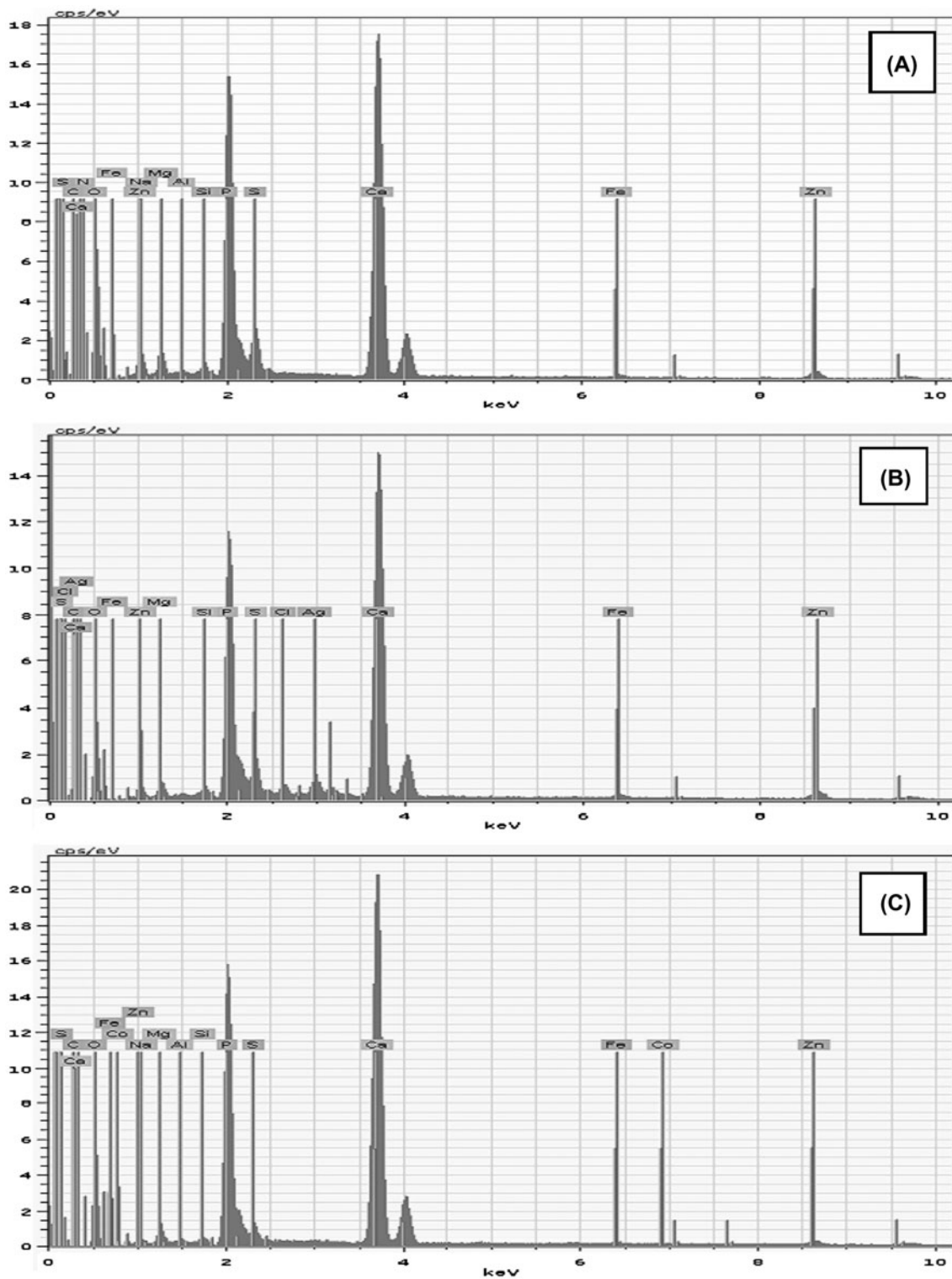


Fig. 7. EDX analysis after scrapping the cake layer; D: cylinder, E: funnel shaped and F: U bundle shaped.

included inorganic materials. Organic substances are lower as compared to the U-shaped module. In addition, the components of the cake were more inorganic

materials. Figs. 4 and 6 indicate that more Ca element was detected in the cake layer in all modules, which cause a more solid and dense cake layer structure.

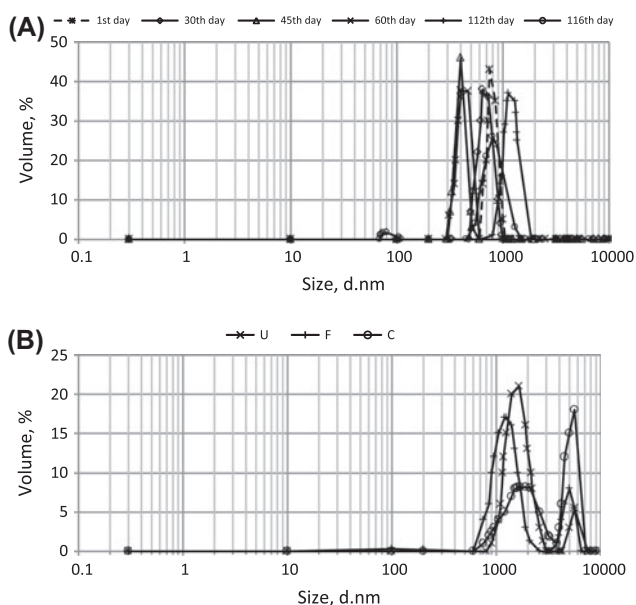


Fig. 8. (A) PSD of mixed liquor; (B) cake layer of membrane modules (U: U-shaped bundle, C: cylinder, F: funnel-shaped) at the end of the operation.

3.4. Particle size distribution

The particle size of bulk sludge mainly distributed between 0.1 and 1 μm and did not change throughout the operation, as seen in Fig. 8(A). On the other hand, the comparison of PSDs in three membrane modules was represented in Fig. 8(B). It can be suggested that the sizes of sludge flocs were smaller than those in the cake sludge flocs in all membrane modules. From Fig. 8(B), two distinct peaks of PSD in the membrane modules appeared ranging from 0.6 to 7 μm . One on them was in the range of 0.6–1.2 μm and the other was in the range of 3–7 μm . The profiles in Fig. 8(B) showed the smaller particles were in the U-shaped module than those in other modules while the more coarse particles were in the cylinder-shaped module. The highest value for R_c was determined in U-shaped module. U-shaped module was considered to have the lowest membrane permeability and also the highest membrane resistance. The small flocs have the priority to attach on membrane surface and imply that small flocs play a key role in cake formation and membrane fouling. Wang et al. [32] observed that gel layer formed on the membrane surface had a smaller PSD compared to bulk sludge. The different behavior in our results obtained with PSD analysis can be attributed to the long-term operation in AnSMBR as 124 days. Long-term continuous compression caused consolidation effect and also the gradual increase of

permeation drag led to the compaction of the internal layer and to the deposition of large particles on membrane surface.

4. Conclusion

In this study, the differences in membrane fouling and filtration performances caused by membrane module designs were observed in AnSMBR used for the treatment of synthetic wastewater. Based on the studies mentioned above, the following conclusions can be drawn:

- The permeate fluxes in the cylinder-shaped module were higher compared with the other modules. Additionally, the highest value for cake layer resistance, R_c , was determined in the case of U-shaped module.
- Both SMP and EPS in cylinder-shaped module were lower than the corresponding values of U-shaped and funnel-shaped modules.
- In the cake layer, more Ca element was detected in all modules which enhance membrane fouling potential of cake layer. On the other hand, the contents of Ca, Mg, Fe, and P were higher in cylinder- and funnel-shaped modules than those in U-shaped modules. Bio-fouling was significantly performed on U-shaped module. Hence, the content of organic substances was found to be lower for U-shaped module than the other membrane modules.
- From the PSD, the sizes of sludge flocs were smaller than those in the cake sludge flocs in all membrane modules. Due to the long-term continuous compression, the consolidation effect generated and the gradual increase of permeation drag led to the compaction of the internal layer and to the deposition of large particles on membrane surface. The smaller particles were in the U-shaped module than those in other modules while the more coarse particles were in the cylinder-shaped module.
- Since the cylinder membrane module showed excellent filtration performances and had low potential of membrane fouling, it was evaluated as the most suitable membrane module to control the membrane fouling in AnSMBR.

Acknowledgment

This study was supported by the Scientific and Technological Research Council of Turkey (TUBITAK) under grant project no. ÇAYDAG-110Y043.

References

- [1] H. Lin, J. Chen, F. Wang, L. Ding, H. Hong, Feasibility evaluation of submerged anaerobic membrane bioreactor for municipal secondary wastewater treatment, *Desalination* 280 (2011) 120–126.
- [2] J. Ho, S. Sung, Methanogenic activities in anaerobic membrane bioreactors (AnMBR) treating synthetic municipal wastewater, *Bioresour. Technol.* 101 (2010) 2191–2196.
- [3] P. Sui, X. Wen, X. Huang, Feasibility of employing ultrasound for on-line membrane fouling control in an anaerobic membrane bioreactor, *Desalination* 219 (2008) 203–213.
- [4] H. Lin, B.Q. Liao, J. Chen, W. Gao, L. Wang, F. Wang, New insights into membrane fouling in a submerged anaerobic membrane bioreactor based on characterization of cake sludge and bulk sludge, *Bioresour. Technol.* 102 (2011) 2373–2379.
- [5] H.J. Lin, K. Xie, B. Mahendran, D.M. Bagley, K.T. Leung, S.N. Liss, B.Q. Liao, Factors affecting sludge cake formation in a submerged anaerobic membrane bioreactor, *J. Membr. Sci.* 361 (2010) 126–134.
- [6] E. Taskan, H. Hasar, Effect of different leachate/acetate ratios in a submerged anaerobic membrane bioreactor, *CLEAN—Soil, Air, Water* 40(5) (2012) 487–492.
- [7] J. Yang, H. Spanjers, J.B. Van Lier, Non-feasibility of magnetic adsorbents for fouling control in anaerobic membrane bioreactors, *Desalination* 292 (2012) 124–128.
- [8] W.J. Gao, H.J. Lin, K.T. Leung, H. Schraft, B.Q. Liao, Structure of cake layer in a submerged anaerobic membrane bioreactor, *J. Membr. Sci.* 374 (2011) 110–120.
- [9] B.Q. Liao, J.T. Kraemer, D.M. Bagley, Anaerobic membrane bioreactors: Applications and research directions, *Crit. Rev. Environ. Sci. Technol.* 36 (2006) 489–530.
- [10] Z. Huang, S.L. Ong, H.Y. Ng, Submerged anaerobic membrane bioreactor for low-strength wastewater treatment: Effect of HRT and SRT on treatment performance and membrane fouling, *Water Res.* 45 (2011) 705–713.
- [11] W.J.J. Gao, H.J. Lin, K.T. Leung, B.Q. Liao, Influence of elevated pH shocks on the performance of a submerged anaerobic membrane bioreactor, *Process Biochem.* 45 (2010) 1279–1287.
- [12] P. Wang, Z. Wang, Z. Wu, S. Mai, Fouling behaviours of two membranes in a submerged membrane bioreactor for municipal wastewater, *J. Membr. Sci.* 382 (2011) 60–69.
- [13] I. Martin-Garcia, V. Monsalvo, M. Pidou, P. Le-Clech, S.J. Judd, E.J. McAdam, B. Jefferson, Impact of membrane configuration on fouling in anaerobic membrane bioreactors, *J. Membr. Sci.* 382 (2011) 41–49.
- [14] H.J. Lin, K. Xie, B. Mahendran, D.M. Bagley, K.T. Leung, S.N. Liss, B.Q. Liao, Sludge properties and their effects on membrane fouling in submerged anaerobic membrane bioreactors (AnSMBR), *Water Res.* 43 (2009) 3827–3837.
- [15] AWWA, WPCF, Standard methods for the examination of water and wastewater (by Arnold E. Greenberg), 18th ed., Washington, DC, 1992.
- [16] T. Li, R. Bai, J. Liu, Distribution and composition of extracellular polymeric substances in membrane-aerated biofilm, *J. Biotechnol.* 135 (2008) 52–57.
- [17] M. Dubois, K.A. Gilles, J.K. Hamilton, P.A. Rebers, F. Smith, Colorimetric method for determination of sugar and related substances, *Anal. Chem.* 28 (1956) 350–356.
- [18] O.H. Lowery, N.J. Rosebrough, A.L. Farr, R.J. Randall, Protein measurement with the Folin phenol reagent, *J. Biol. Chem.* 193 (1951) 265–275.
- [19] X. Zhang, Z. Wang, Z. Wu, F. Lu, J. Tong, L. Zang, Formation of dynamic membrane in an anaerobic membrane bioreactor for municipal wastewater treatment, *Chem. Eng. J.* 165 (2010) 175–183.
- [20] N. Jang, X. Ren, G. Kim, C. Ahn, J. Cho, I. Kima, Characteristics of soluble microbial products and extracellular polymeric substances in the membrane bioreactor for water reuse, *Desalination* 202 (2006) 90–98.
- [21] F. Meng, H. Zhang, F. Yang, L. Liu, Characterization of cake layer in submerged membrane bioreactor, *Environ. Sci. Technol.* 41 (2007) 4065–4070.
- [22] P. Le-Clech, Y. Marselina, R. Stuetz, V. Chen, Fouling visualisation of soluble microbial product models in MBRs, *Desalination* 199 (2006) 477–479.
- [23] C. Fersi, L. Gzara, M. Dhahbi, Flux decline study for textile wastewater treatment by membrane processes, *Desalination* 244 (2009) 321–332.
- [24] K.-H. Choo, C.-H. Lee, Membrane fouling mechanisms in the membrane-coupled anaerobic bioreactor, *Water Res.* 30 (1996) 1771–1780.
- [25] A.P. Trzcinski, D.C. Stuckey, Treatment of municipal solid waste leachate using a submerged anaerobic membrane bioreactor at mesophilic and psychrophilic temperatures: Analysis of recalcitrants in the permeate using GC-MS, *Water Res.* 44 (2010) 3671–3680.
- [26] X. Huang, R. Liu, Y. Qian, Behaviour of soluble microbial products in a membrane bioreactor, *Process Biochem.* 36 (2000) 401–406.
- [27] W. Lee, S. Kang, H. Shin, Sludge characteristics and their contribution to microfiltration in submerged membrane bioreactors, *J. Membr. Sci.* 216 (2003) 217–227.
- [28] S. Liang, C. Liu, L.F. Song, Soluble microbial products in membrane bioreactor operation: Behaviors, characteristics, and fouling potential, *Water Res.* 41 (2007) 95–101.
- [29] S. Tsuneda, H. Aikawa, H. Hayashi, A. Yuasa, A. Hirata, Extracellular polymeric substances responsible for bacterial adhesion onto solid surface, *FEMS Microbiol. Lett.* 223 (2003) 287–292.
- [30] A. Pollice, A. Brookes, B. Jefferson, S. Budd, Sub-critical flux fouling in membrane bioreactors—review of recent literature, *Desalination* 174 (2005) 221–230.
- [31] M. Dagnew, Characterization of anaerobic membrane digesters for stabilization of waste activated sludge, PhD thesis, Civil Engineering, Waterloo, Ontario, Canada, 2010.
- [32] Z. Wang, Z. Wu, X. Yin, L. Tian, Membrane fouling in a submerged membrane bioreactor (MBR) under sub-critical flux operation: Membrane foulant and gel layer characterization, *J. Membr. Sci.* 325 (2008) 238–244.